

Scattering Functions for Disordered Two-Component Polymer Systems Including Block Polymers

Keiji Mori,[†] Hideaki Tanaka, and Takeji Hashimoto*

Department of Polymer Chemistry, Faculty of Engineering, Kyoto University, Kyoto 606, Japan. Received July 15, 1986

ABSTRACT: Scattering functions $I(q)$ for various binary polymer mixtures in the disordered state are presented. The calculations of the scattering functions involve evaluations of $S(q)/W(q)$ for particular systems of interest in the general equation developed by Leibler ($I(q)^{-1} \sim [S(q)/W(q) - 2\chi]$). The systems to be covered include (i) block polymers comprising random copolymers ABR1 and ABR2, where ABR1 and ABR2 are random copolymers of A and B monomers with different compositions and degrees of polymerization (ABR1-ABR2), (ii) mixtures of block polymers ABR1-ABR2 and ABR3-ABR4, where ABR I ($I = 1-4$) represents a random copolymer (ABR1-ABR2 + ABR3-ABR4), and (iii) ternary mixtures of A-B diblock polymer, A homopolymer, and B homopolymer (A-B + A + B) with a finite value of χ , the thermodynamic interaction parameter between A and B. The formulas obtained for cases i and ii cover almost all the binary systems as special cases. The scattering behaviors are numerically calculated for some typical cases, from which the spinodal points $(\chi N)_s$ and the wavelengths ξ of the dominant mode of the thermal concentration fluctuations are predicted for the typical systems. Finally, the predicted scattering profiles are compared with the measured profiles. Good agreement is found between the measured and predicted scattering profiles.

I. Introduction

The elastic scattering of light, X-rays, and neutrons due to thermal concentration fluctuations in binary polymer systems in the disordered state (i.e., in the single-phase regime) is one of the interesting subjects in polymer physics because the fluctuations reflect, in principle, properties of single polymer molecules such as their radius of gyration and thermodynamic interactions χ between the constituent component polymers.¹ The analyses also lead to the prediction of the phase transition in the binary mixtures.

To date, one of the most general theories for binary polymer mixtures in the disordered state was presented by Leibler² in the context of the *random phase approximation* (RPA).³ For example, the theory predicts the elastic scattering intensity $I(q)$ as a function of scattering vector q

$$I(q) \sim [S(q)/W(q) - 2\chi]^{-1} \quad (\text{I-1})$$

where

$$q = (4\pi/\lambda) \sin(\theta/2) \quad (\text{I-2})$$

λ and θ are the wavelength of the incident beam and the scattering angle, respectively. The functions $S(q)$ and $W(q)$ are given by

$$S(q) = S_{AA}(q) + S_{BB}(q) + 2S_{AB}(q) \quad (\text{I-3})$$

$$W(q) = S_{AA}(q)S_{BB}(q) - S_{AB}^2(q) \quad (\text{I-4})$$

The functions of $S_{KJ}(q)$ ($K, J, = A$ or B) are the Fourier transform of the density-density correlation for K and J monomers in a given polymer chain.

The correlations $S_{KJ}(q)$ and the function $S(q)/W(q)$ were presented by Leibler² for A-B diblock polymer and by Leibler and Benoit⁴ for binary mixtures of A-B and A (or B) monomers, from which one can predict the scattering profiles for these systems. One can determine the wavelength ξ of the dominant mode of the thermal concentration fluctuations and the spinodal points χ_s for the systems

$$\xi = 2\pi/q_m \quad (\text{I-5})$$

$$I(q_m)^{-1} \sim S(q_m)/W(q_m) - 2\chi_s = 0 \quad (\text{I-6})$$

In eq I-5, q_m is the value q at which $I(q)$ becomes maximum or $S(q)/W(q)$ becomes minimum, and χ_s is the χ parameter

at the spinodal point. Equation I-6 gives a criterion for the spinodal point for the order-disorder transition¹ in block polymers where the scattered intensity at $q = q_m \sim 1/R_g$ ($I(q_m)$) diverges to infinity. More precise definitions of the spinodal points for mixtures with block polymers as at least one component will be discussed in section IV (eq IV-1 and IV-2).

Since eq I-1 is the general equation applicable for any binary polymer system in the context of the RPA, the remaining problems exist in calculating the function $S(q)/W(q)$ for the systems of one's interests and critically investigating the validity of the theory for each system of one's interests.

In this paper, we first present a brief overview of existing theories (section II). We then present scattering formulas for $S(q)/W(q)$ and consequently for $I(q)$ for two major systems (section III):

(i) *Block Polymers Constituted of Random Copolymers of A and B Monomers, Designated ABR, with Different Compositions of A and Degrees of Polymerization.* We designate such block polymers based on the random copolymers as ABR1-ABR2, R designating a random copolymer.²⁹ Before we advance discussions about the random copolymers, it is important to note that the random copolymer that we deal with in this paper strictly corresponds to the random copolymer poly(A-ran-B) defined by the IUPAC Commission on Macromolecular Nomenclature.²⁵ The sequence length distribution of A and B monomers in the random copolymer should obey Bernoulli statistics: i.e., the probability of finding A monomer in a given sequence is independent of the type of the monomers in its nearest neighbors. The probability of finding a particular sequence $P[\dots ABA \dots]$ is given in terms of a probability of finding A monomers $P[A]$

$$P[\dots ABA \dots] = \prod_{i=A,B,A,\dots} P[i]$$

Therefore the sequence length distribution of A (or B) is given by a most probable distribution

$$\langle N \rangle_w / \langle N \rangle_n = 2 \quad (\text{I-7})$$

where $\langle N \rangle_w$ and $\langle N \rangle_n$ are the weight- and number-average sequences of A or B in the random copolymers. Although the random copolymer is only a special case of the statistical copolymers²⁵ to which the most of the real copolymers correspond, it should be quite useful and informative to compare the behaviors of the real copolymers

[†] Present address: Research Center, Toyobo Co. Ltd., Katata, Ohtsu, Shiga 520-02, Japan.

Table I
List of Theories on the Scattering from Disordered
Mixtures and Block Polymers

authors	ref	remarks
de Gennes	3	mixtures of A and B homopolymers with $\chi \neq 0$
Boue et al.	10	HPS-DPS-HPS triblock polymers with $\chi = 0$
LeGrand and LeGrand	11	A-B, A-B-A, -(A-B) _n - block polymers with $\chi = 0$
Leibler	2	general scattering theory for binary systems and detailed formula for A-B diblock polymers with $\chi \neq 0$
Leibler and Benoit	4	mixtures of A-B diblock polymer and A homopolymer and chemical polydispersity in A-B diblock polymers with $\chi = 0$
Benmouna and Benoit	9	polymer solution and block polymer solution with $\chi \neq 0$ based on extension of Ornstein and Zernike

with those of the random copolymers.

(ii) *Mixtures of the Block Polymer ABR1-ABR2 and Another Block Polymer ABR3-ABR4*. These two systems (i) and (ii) generally cover almost all binary systems of interest, in the sense discussed in section III. Mixtures involving random copolymers and statistical copolymers, or, more generally, copolymers, are known to be of practical importance in determining the "miscibility window"⁵⁻⁷ and are expected to be widely used in miscibility studies and in the study of phase separation kinetics⁸ of polymer blends.

In section IV we present results of numerical solutions of the scattering profiles, the spinodal points χ_s , and the wavelengths ξ for (i) mixtures of pure block polymers A-B1 and A-B2, where A-B1 and A-B2 are the diblock polymer consisting of polymers A and B (section 4-1), (ii) ternary mixtures consisting of A-B, A, and B (section 4-2), (iii) triblock polymers A-B-A (section 4-3) in comparison with A-B, and (iv) mixtures in disordered states that form a single phase and those that form two coexisting liquid phases (section 4-4). Finally, in section V we compare theoretical and experimental scattering profiles.

II. Review of Existing Theories

2-1. Various Theories and Remaining Problems. In this section we briefly review theories describing the scattering from binary polymer systems in the disordered state. Except for the theory of Benmouna and Benoit,⁹ all of the theories describe the scattering from the bulk disordered state in the context of the RPA.³

A list of the theories is given in Table I.²⁶ de Gennes³ presented first the scattering theory of binary polymer mixtures A/B with a nonzero thermodynamic interaction parameter χ . The first scattering theory for the block polymer was presented by Boue et al. for HPS-DPS-HPS, assuming a zero χ value¹⁰ (HPS and DPS denote protonated polystyrene (PS) and deuteriated PS, respectively). LeGrand and LeGrand¹¹ then conducted similar calculations to describe the scattering from A-B diblock polymers, A-B-A triblock polymers, and -(A-B)_n- multiblock polymers, again assuming a zero χ value.

Leibler² proposed a general equation (eq I-1) and presented the scattering equation for A-B diblock polymer with nonzero χ . This equation predicts an effect of χ and can be applied to describe generally the scattering from mixtures and all block polymers composed of two types of monomers A and B, provided that appropriate functions for $S(q)/W(q)$ can be calculated. The calculations by LeGrand and LeGrand¹¹ and Boue et al.¹⁰ correspond to

those for $[S(q)/W(q)]^{-1}$. Leibler and Benoit⁴ further extended the theory to describe the scattering from mixtures of A-B diblock polymer and A (or B) homopolymer, and, as a special case of the mixtures, they dealt with the problem of "chemical polydispersity" (i.e., the distribution of the chemical composition of A (or B) in A-B).

A fundamental feature of the multicomponent mixtures is described in eq II-1⁴ for S_{AA} , for example, which is the Fourier transform of the density-density correlation for A segments in the mixture and which appears as one of the terms in $S(q)/W(q)$ in eq I-1

$$S_{AA}(q) = \sum_m \frac{\phi_m}{N_m} \sum_{ij} \mu_i \mu_j P_{ij}(q) = \sum_m \phi_m S_{AAm}(q) \quad (\text{II-1})$$

where ϕ_m is the volume fraction of the m th polymer (A (or B) homopolymer, A-B diblock polymer, etc.). Here again we consider the cases where any component polymers consist of monomers A and/or B. N_m is the degree of polymerization of the m th polymer. $P_{ij}(q)$ is the Fourier transform of the density-density correlation between the i th and j th segments for Gaussian coils, and μ_i is unity if the i th segment is A monomer and zero if it is B monomer. $S_{AAm}(q)$ is the density-density correlation between the two A monomers for the m th polymer. Equation II-1 is again general, applicable to any kind of multicomponent mixture in which the component polymers consist of monomers A and/or B. In the Leibler-Benoit case⁴ the index m is the m th A-B diblock polymer with N_m and f_m , f_m being the fraction of A in the m th A-B diblock polymer. How f_m is related to S_{AA} , S_{AB} , and S_{BB} and the detailed calculation procedures are well described in the papers by Leibler² and Leibler and Benoit⁴ and will not be repeated in this paper.

Consequently by combining eq I-1 and II-1 one can generally calculate any binary mixture. The remaining problem exists only in calculating appropriate functional forms of $S(q)/W(q)$ for the systems of one's interests. In fact, we shall present the scattering formulas for the diblock polymer ABR1-ABR2, in which ABR1 and ABR2 are random copolymers of monomers A and B, i.e., poly-(A-*ran*-B), and for mixtures of the two block polymers ABR1-ABR2 and ABR3-ABR4, the latter being another block polymer whose constituent blocks are random copolymers of monomers A and B. The two block polymers ABR1-ABR2 and ABR3-ABR4 differ in polymerization indices (N_1 and N_2) and fraction of one block (f_1 and f_2). The fraction of A monomers in ABR_I ($I = 1-4$), defined as ψ_I , is also different, as shown in Figure 3. Needless to say, experimental work is needed to critically test the theories. Part of this work is presented in section V, and further work will be presented in our future publications.¹³⁻¹⁵

Benmouna and Benoit⁹ described the scattering function by using the Ornstein-Zernike approach, instead of using the RPA, and clearly showed that in the case of polymer A being moderately dilute and B being solvent, their equation reduces to Zimm's equation, while in the case of B being polymer, their equation reduces to the equations derived by de Gennes³ and Leibler² based upon the RPA.

2-2. Scattering Profiles. Figure 1 shows typical scattering profiles for binary mixtures of A and B and those for A-B diblock polymers²⁴ with different values of χN calculated respectively from the equations derived by de Gennes³ and Leibler.² Polymers A and B are assumed to be symmetric with degrees of polymerization $N_A = N_B = N$ and with Kuhn statistical segment lengths $a_A = a_B = a$, and the relative intensity $I(q)$ was normalized with respect to N . R_g is the radius of gyration of polymers A and B,²⁴ $R_g^2 = Na^2/6$.

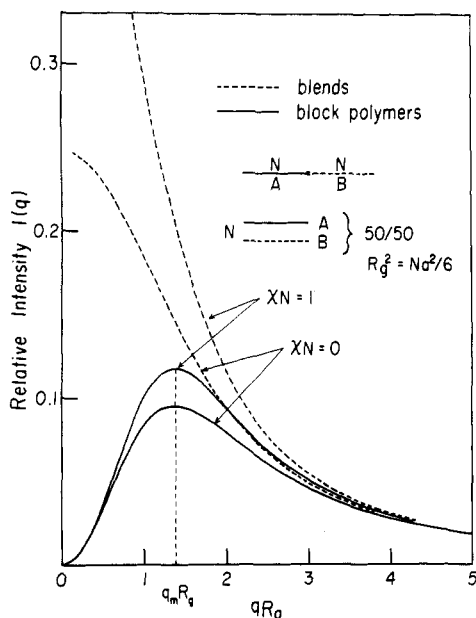


Figure 1. Comparison of the elastic scattering profiles of A-B block polymers (solid curves) and polymer mixtures of A and B homopolymers (broken curves) in the disordered state for two values of the interaction parameter χ ($\chi N = 0$ and $\chi N = 1.0$). N is the degree of polymerization of the A and B polymers, and a is the Kuhn statistical segment length of the polymers. q is the scattering vector, given by $q = (4\pi/\lambda) \sin(\theta/2)$, where θ is the scattering angle.

One can see that the scattering profiles for the A/B mixtures are dramatically different from those for the A-B block polymers, especially at small $q < q_m$, q_m being the q value at which the scattering intensity becomes maximum for the block polymer.

$$q_m = 0 \quad \text{for A/B mixtures} \quad (\text{II-2})$$

but

$$q_m \sim 2^{1/2}/R_g \quad \text{for A-B block polymers}^{24} \quad (\text{II-3})$$

For A/B mixtures, the smaller the q 's, the smaller is the "gradient free energy".¹⁶ Hence the smaller the q 's, the smaller is the free energy of the q -Fourier component of the fluctuations $F(q)$ with unit intensity $|\eta_q|^2 = 1$, where η_q is the amplitude of the q -Fourier component of the fluctuation. Since $I(q)$ is related to susceptibility $1/F(q)$

$$I(q) \sim k_B T / F(q) \quad (\text{II-4})$$

and $F(q)$ is minimum at $q = 0$, $I(q)$ becomes maximum at $q = 0$ for an A/B mixture. On the other hand, in the case of block polymer, $F(q)$ is modified by the molecular connection between A and B in A-B diblock polymers, and in order to generate the thermal concentration fluctuations with wavenumber $q < q_m$ and with a given η_q , e.g., $|\eta_q|^2 = 1$, the A and B chains have to be stretched because of the molecular connectivity.¹² That is, in the case of block polymers, modes of fluctuations must be strongly coupled with conformation of the chains because of the connectivity. Such coupling is not necessarily involved in A/B mixtures. The smaller the q , the larger the stretching should be, which results in a greater conformational entropy loss in the disordered state and hence in greater free energy $F(q)$. Consequently $I(q)$ decreases with decreasing q , approaching zero when q goes to zero.

One can see also in Figure 1 that q_m is independent of χ and therefore of temperature but the intensity decreases with decreasing χN . These apply for both mixtures and block polymers.

ABR1	ABR2	
Nf	N(1-f)	N (DP)
ψ_1	ψ_2	A-monomer fraction
$1-\psi_1$	$1-\psi_2$	B-monomer fraction

Figure 2. Definitions of the parameters N , ψ_1 , ψ_2 , and f in the block polymer ABR1-ABR2 based on the random copolymers ABR1 and ABR2. N is the total degree of polymerization (DP), ψ_1 and ψ_2 are the fractions of A monomers in the random copolymers ABR1 and ABR2, respectively, and f is the fraction of ABR1 in the block polymer.

Table II
Various Cases Covered by ABR1-ABR2 Block Polymers

1. $0 < \psi_1, \psi_2 < 1$	ABR1-ABR2
2. $\psi_1 = 1, \psi_2 = 0$	A-B
3. $0 < \psi_1 < 1, \psi_2 = 1$	ABR1-A
4. $0 < \psi_1 < 1, \psi_2 = 0$	ABR1-B

Table III
Various Cases Covered by ABR1-ABR2 + ABR3-ABR4

1. $0 < \phi_1 < 1$	ABR1-ABR2 + ABR3-ABR4
2. $\phi_1 = 1$ (or 0)	ABR1-ABR2 (or ABR3-ABR4)
3. $f_2 = 1$ (or 0)	ABR1-ABR2 + ABR3 (or ABR4)
4. $f_1 = f_2 = 1$	ABR1 + ABR3

Table IV
Various Cases Covered by Table III-1: ABR1-ABR2 + ABR3-ABR4

$0 < \psi_1, \psi_2, \psi_3, \psi_4 < 1$	ABR1-ABR2 + ABR3-ABR4
$\psi_1 = 1, 0 < \psi_2, \psi_3, \psi_4 < 1$	A-ABR2 + ABR3-ABR4
$\psi_2 = 0, 0 < \psi_1, \psi_3, \psi_4 < 1$	ABR1-B + ABR3-ABR4
$\psi_1 = \psi_3 = 1, 0 < \psi_2, \psi_4 < 1$	A-ABR2 + A-ABR4
$\psi_1 = 1, \psi_4 = 0, 0 < \psi_2, \psi_3 < 1$	A-ABR2 + ABR3-B
$\psi_1 = 1, \psi_2 = 0, 0 < \psi_3, \psi_4 < 1$	A-B + ABR3-ABR4
$\psi_1 = \psi_3 = 1, \psi_2 = 0, 0 < \psi_4 < 1$	A-B + A-ABR4
$\psi_1 = 1, \psi_2 = \psi_4 = 0, 0 < \psi_3 < 1$	A-B + ABR3-B
$\psi_1 = \psi_3 = 1, \psi_2 = \psi_4 = 0$	A-B + A-B

Table V
Various Cases Covered by A-B + A-B ($\psi_1 = \psi_3 = 1, \psi_2 = \psi_4 = 0$)

1. $0 < \phi_1 < 1$	A-B + A-B
2. $\phi_1 = 1$ (or 0)	A-B
3. $f_1 = 1$ (or 0)	A (B) + A-B
4. $f_1 = 1, f_2 = 0$ (or $f_1 = 0, f_2 = 1$)	A + B

III. Scattering Functions

In this section we first discuss the motivation for the studies (section 3-1). Then we present formulas for $S(q)/W(q)$ for the block polymers ABR1-ABR2 (section 3-2) and mixtures of the two block polymers (ABR1-ABR2 and ABR3-ABR4) (section 3-3), ternary mixtures of A-B, A, and B (section 3-4), and A-B-A triblock polymers (section 3-5).

3-1. Motivation. The calculation of the function $S(q)/W(q)$ associated with $I(q)$ for ABR1-ABR2 covers most generally any kind of diblock polymer by changing ψ_1 and ψ_2 (Table II). The parameters associated with this diblock polymer are shown in Figure 2. Similarly, the calculation of the function for the mixtures of the diblock polymers ABR1-ABR2 and ABR3-ABR4 covers most generally the various kinds of binary mixtures as summarized in Table III, the related parameters being summarized in Figure 3. Moreover, each of the cases 1-4 in Table III contains many possible cases, depending on the values ψ_1 and ψ_2 . For example, Table IV summarizes the various cases covered by a special case (case 1) of Table III. Alternatively, by setting $\psi_1 = \psi_3 = 1$ and $\psi_2 = \psi_4 = 0$ in Table IV, one can have special cases as summarized

ABR1		ABR2		Vol. fraction in the mixtures ϕ_1
$f_1 N_1$	$(1-f_1)N_1$	N_1 (DP)		
ψ_1	ψ_2	A-monomer	fraction	
$1-\psi_1$	$1-\psi_2$	B-monomer		
ABR3		ABR4		ϕ_2 ($\phi_1 + \phi_2 = 1$)
$f_2 N_2$	$(1-f_2)N_2$	N_2 (DP)		
ψ_3	ψ_4	A-monomer	fraction	
$1-\psi_3$	$1-\psi_4$	B-monomer		

Figure 3. Definitions of the parameters $N_1, \psi_1, \psi_2, f_1, N_2, \psi_3, \psi_4, f_2, \phi_1$, and ϕ_2 in binary mixtures of the block polymers ABR1-ABR2 and ABR3-ABR4. N_i, ψ_i , and f_i correspond to the parameters defined in Figure 2, and ϕ_1 is the volume fraction of the block polymer ABR1-ABR2 in the binary mixture.

in Table V. In this section we first present in sections 3-2 and 3-3 the formulas $I(q)$ and $S(q)/W(q)$ for the general cases. The formulas for ternary mixtures of A-B, A, and B and that for A-B-A triblock polymers do not correspond to the special cases treated in sections 3-2 and 3-3 and hence will be given separately in sections 3-4 and 3-5, respectively. Numerical solutions for the scattering profiles will be given in section IV for the special cases described in Table V and for the ternary mixtures and A-B-A triblock polymers.

3.2. Scattering Formula for Random-Copolymer-Based Block Polymers: ABR1-ABR2. Here we present a formula for $S(q)/W(q)$ in eq I-1 for the diblock polymer ABR1-ABR2. By following the same calculational procedure as developed by Leibler and by using the random phase approximation, the $S_{IJ}(q)$'s ($I, J = A, B$) in eq I-3 and I-4 are given by

$$S_{AA}(q) = \psi_1^2 Ng(f, N) + \psi_2^2 Ng(1-f, N) + \psi_1 \psi_2 N [g(1, N) - g(f, N) - g(1-f, N)] \quad (\text{III-1})$$

$$S_{BB}(q) = (1 - \psi_1)^2 Ng(f, N) + (1 - \psi_2)^2 Ng(1-f, N) + (1 - \psi_1)(1 - \psi_2) N [g(1, N) - g(f, N) - g(1-f, N)] \quad (\text{III-2})$$

$$S_{AB}(q) = \psi_1(1 - \psi_1) Ng(f, N) + \psi_2(1 - \psi_2) Ng(1-f, N) + \frac{1}{2} [\psi_1(1 - \psi_2) + \psi_2(1 - \psi_1)] N [g(1, N) - g(f, N) - g(1-f, N)] \quad (\text{III-3})$$

where

$$g(f, N) \equiv (2/x^2) [(fx - 1) + \exp(-fx)] \quad (\text{III-4})$$

and

$$x \equiv q^2 Na^2 / 6 \quad (\text{III-5})$$

The quantity a is the statistical segment length for ABR1 and ABR2 (assumed to be identical), and N, f , and ψ_i are defined in Figure 2, f being the fraction of ABR1 in the block polymer ABR1-ABR2. A more precise description of the calculational procedures will be given in the Appendix.

From eq I-1 to I-4 and III-1 to III-5, the formula for the scattered intensity $I(q)$ can be summarized as follows:

$$I(q) \sim \frac{N(b_A - b_B)_{\text{eff}}^2}{F(q) - 2\chi_{\text{eff}}N} \quad (\text{III-6})$$

where

$$F(q) = g(1, N) \{ g(f, N) g(1-f, N) - \frac{1}{4} [g(1, N) - g(f, N) - g(1-f, N)]^2 \}^{-1} \quad (\text{III-7})$$

$F(q)$ corresponds to

$$F(q) = NS(q)/W(q) \quad (\text{III-8})$$

for pure A-B diblock polymer.² The quantity χ_{eff} in eq III-6 is the *effective interaction parameter*, defined by

$$\chi_{\text{eff}} = \chi(\psi_1 - \psi_2)^2 \quad (\text{III-9})$$

where χ is the bare interaction parameter between homopolymers A and B. The quantity $(b_A - b_B)_{\text{eff}}$ in eq III-6 is the *effective scattering contrast*, defined by

$$(b_A - b_B)_{\text{eff}}^2 = (b_A - b_B)^2 (\psi_1 - \psi_2)^2 \quad (\text{III-10})$$

where $(b_A - b_B)$ is the bare scattering contrast between the pure polymers A and B. Therefore the *interaction* of two block sequences ABR1 and ABR2 in ABR1-ABR2 is *diluted* relative to that for A and B in pure A-B block polymer by an amount $(\psi_1 - \psi_2)^2$, which is due to incorporation of the unlike monomers B and A in A and B block sequences, respectively. Similarly, the scattering contrast is diluted by an amount $(\psi_1 - \psi_2)^2$. Note that $0 < (\psi_1 - \psi_2)^2 < 1$ for the random-copolymer-based block polymers from the definitions of ψ_1 and ψ_2 given in Figure 2.

From eq III-6, the spinodal point is found at $(\chi_{\text{eff}}N)_s$, satisfying

$$F(q_m) = 2(\chi_{\text{eff}}N)_s \quad (\text{III-11})$$

$$= 2(\chi N)_s (\psi_1 - \psi_2)^2 \quad (\text{III-12})$$

where q_m is q at which $F(q)$ becomes minimum. The incorporation of the unlike monomers in each block sequence in ABR1-ABR2 increases $(\chi N)_s$ by a factor $(\psi_1 - \psi_2)^{-2}$ ($(\psi_1 - \psi_2)^{-2} > 1$), resulting in an *enhancement of the miscibility*, since $F(q_m)$ is independent of $(\psi_1 - \psi_2)^2$.

The scattering intensity $I(q)$ for ABR1-B and A-ABR2 is obtained by setting $\psi_2 = 0$ and $\psi_1 = 1$, respectively.

For pure A-B block polymer, for which $\psi_1 = 1$ and $\psi_2 = 0$, eq III-6 reduces to the formula derived by Leibler; i.e.

$$I(q) \sim \frac{N(b_A - b_B)^2}{F(q) - 2\chi N} \quad (\text{III-13})$$

Hence the scattering formula for the random-copolymer-based block polymers (eq III-6) is obtained from that for the ideal block polymer (eq III-13) by substituting the interaction parameter χ by χ_{eff} and the scattering contrast $(b_A - b_B)$ by $(b_A - b_B)_{\text{eff}}$.

3.3. Scattering Formula for Mixtures of the Block Polymers: ABR1-ABR2 + ABR3-ABR4. The quantities S_{AA}, S_{AB} , and S_{BB} in eq I-1, I-3, and I-4 are given from eq II-1 by

$$S_{IJ} = \phi_1 S_{IJ1} + (1 - \phi_1) S_{IJ2} \quad (I, J = A, B) \quad (\text{III-14})$$

where the terms S_{IJ1} (S_{IJ2}) correspond to those for ABR1-ABR2 (ABR3-ABR4); i.e.

$$S_{AA} = \phi_1 S_{AA1} + (1 - \phi_1) S_{AA2} \quad (\text{III-15})$$

$$S_{BB} = \phi_1 S_{BB1} + (1 - \phi_1) S_{BB2} \quad (\text{III-16})$$

$$S_{AB} = \phi_1 S_{AB1} + (1 - \phi_1) S_{AB2} \quad (\text{III-17})$$

$$S_{AAi} = \psi_{1+2(i-1)}^2 N_i g(f_i, N_i) + \psi_{2+2(i-1)}^2 N_i g(1-f_i, N_i) + \psi_{1+2(i-1)} \psi_{2+2(i-1)} N_i [g(1, N_i) - g(f_i, N_i) - g(1-f_i, N_i)] \quad (i = 1, 2) \quad (\text{III-18})$$

$$S_{BBi} = (1 - \psi_{1+2(i-1)})^2 N_i g(f_i, N_i) + (1 - \psi_{2+2(i-1)})^2 N_i g(1-f_i, N_i) + (1 - \psi_{1+2(i-1)})(1 - \psi_{2+2(i-1)}) N_i [g(1, N_i) - g(f_i, N_i) - g(1-f_i, N_i)] \quad (i = 1, 2) \quad (\text{III-19})$$

$$S_{ABi} = \psi_{1+2(i-1)}(1 - \psi_{1+2(i-1)}) N_i g(f_i, N_i) + \psi_{2+2(i-1)}(1 - \psi_{2+2(i-1)}) N_i g(1-f_i, N_i) + \frac{1}{2} [\psi_{1+2(i-1)}(1 - \psi_{2+2(i-1)}) + \psi_{2+2(i-1)}(1 - \psi_{1+2(i-1)})] N_i [g(1, N_i) - g(f_i, N_i) - g(1-f_i, N_i)] \quad (i = 1, 2) \quad (\text{III-20})$$

The scattered intensity is calculated from eq I-1, I-3, I-4, and III-15 to III-20.

In the special case of binary mixtures of pure block polymers A-B with f_1 and N_1 and A-B with f_2 and N_2 , for which $\psi_1 = \psi_3 = 1$ and $\psi_2 = \psi_4 = 0$, one obtains from eq III-15 to III-20

$$S_{AA} = \phi_1 N_1 g(f_1, N_1) + (1 - \phi_1) N_2 g(f_2, N_2) \quad (\text{III-21})$$

$$S_{BB} = \phi_1 N_1 g(1 - f_1, N_1) + (1 - \phi_1) N_2 g(1 - f_2, N_2) \quad (\text{III-22})$$

$$S_{AB} = \frac{1}{2} \{ \phi_1 N_1 [g(1, N_1) - g(f_1, N_1) - g(1 - f_1, N_1)] + (1 - \phi_1) N_2 [g(1, N_2) - g(f_2, N_2) - g(1 - f_2, N_2)] \} \quad (\text{III-23})$$

The intensity can be calculated from eq I-1, I-3, I-4, and III-21 to III-23.

Let us consider further the special case of the binary mixture of pure A-B block polymers. When $f_1 = 1$ and $f_2 = 0$, the system reduces to a binary mixture of homopolymers A and B. Noting that in eq III-4

$$g(0, N_1) = g(0, N_2) = 0 \quad (\text{III-24})$$

one obtains from eq III-21 to III-23

$$S_{AA} = \phi_1 N_1 g(1, N_1) \quad (\text{III-25})$$

$$S_{BB} = (1 - \phi_1) N_2 g(1, N_2) \quad (\text{III-26})$$

$$S_{AB} = 0 \quad (\text{III-27})$$

Hence one obtains from eq I-3 and I-4

$$S(q) = \phi_1 N_1 g(1, N_1) + (1 - \phi_1) N_2 g(1, N_2) \quad (\text{III-28})$$

$$W(q) = \phi_1 (1 - \phi_1) N_1 N_2 g(1, N_1) g(1, N_2) \quad (\text{III-29})$$

From eq I-1, III-28, and III-29, one obtains the equation given by de Gennes³

$$I(q)^{-1} \sim \frac{1}{\phi_1 N_1 g(1, N_1)} + \frac{1}{(1 - \phi_1) N_2 g(1, N_2)} - 2\chi \quad (\text{III-30})$$

Moreover, if $N_1 = N_2 = N$ so that $g(1, N_1) = g(1, N_2) \equiv g(N)$ and $\chi = 0$, one obtains

$$I(q) \sim \phi_1 (1 - \phi_1) N g(N) \quad (\text{III-31})$$

This is an equation³ from which one can extract the molecular scattering $g(N)$ for bulk polymers containing deuterium-labeled chains.

3-4. Ternary Mixtures: A-B + A + B. The scattering formula for ternary mixtures of A-B diblock polymer, A homopolymer, and B homopolymer can easily be obtained by extending the basic equations III-21 to III-23 for binary mixtures to ternary systems. If the fraction of A component and total degree of polymerization of each constituent polymer are defined as f_1 and N_1 , f_2 and N_2 , and f_3 and N_3 , respectively, and the fraction of each constituent polymer in the ternary mixture is defined as ϕ_1 , ϕ_2 , and ϕ_3 , where $\phi_1 + \phi_2 + \phi_3 = 1$ (see Figure 4), one obtains from eq II-1

$$S_{AA} = \phi_1 N_1 g(f_1, N_1) + \phi_2 N_2 g(1, N_2) + \phi_3 N_3 g(0, N_3) \\ = \phi_1 N_1 g(f_1, N_1) + \phi_2 N_2 g(1, N_2) \quad (\text{III-32})$$

$$S_{BB} = \phi_1 N_1 g(1 - f_1, N_1) + \phi_2 N_2 g(0, N_2) + \phi_3 N_3 g(1, N_3) \\ = \phi_1 N_1 g(1 - f_1, N_1) + \phi_3 N_3 g(1, N_3) \quad (\text{III-33})$$

$$S_{AB} = \frac{1}{2} \{ \phi_1 N_1 [g(1, N_1) - g(f_1, N_1) - g(1 - f_1, N_1)] + \\ \phi_2 N_2 [g(1, N_2) - g(1, N_2) - g(0, N_2)] + \phi_3 N_3 [g(1, N_3) - \\ g(0, N_3) - g(1, N_3)] \} = \\ \frac{1}{2} \phi_1 N_1 [g(1, N_1) - g(f_1, N_1) - g(1 - f_1, N_1)] \quad (\text{III-34})$$

The intensity formula is obtained from eq I-1, I-3, I-4, and III-32 to III-34.

A	B	fraction	DP
$f_1 N_1$	$(1 - f_1) N_1$	ϕ_1	N_1
A			
	$f_2 = 1, 1 - f_2 = 0, N_2$	ϕ_2	N_2
	B		
	$f_3 = 0, 1 - f_3 = 1, N_3$	ϕ_3	N_3

Figure 4. Definitions of the parameters f_i , N_i , and ϕ_i in the ternary mixture of A-B, A, and B.

3-5. A-B-A Triblock Polymers. If the fraction of each block sequence in A-B-A triblock polymer is f_1 , f_2 , and f_3 , respectively, and the total degree of polymerization of the block polymer is N , then

$$S_{AA} = N [g(f_1, N) + g(f_2, N) + g(f_3, N) + g(1, N) - \\ g(1 - f_3, N) - g(1 - f_1, N)] \quad (\text{III-35})$$

$$S_{BB} = N g(f_2, N) \quad (\text{III-36})$$

$$S_{AB} = \\ \frac{1}{2} N [g(1 - f_1, N) + g(1 - f_3, N) - g(f_1, N) - g(f_3, N) - 2g(f_2, N)] \quad (\text{III-37})$$

In the case of $f_3 = 0$, the equation reduces to the case of diblock polymer.

IV. Numerical Calculations of Scattering Profiles and Discussion of the Results

In this section we present calculated scattering profiles for various systems for the case of $\chi = 0$. Although the case of $\chi = 0$ corresponds to a special case where there is no excess interaction energy upon mixing, the numerical calculations of the scattering profiles for this case give important information such as the wavelength ξ of the dominant thermal concentration fluctuations and the spinodal point χ_s . The wavelength ξ is obtained from eq I-5, and χ_s is obtained from a minimum of the function $S(q)/W(q)$. In the case of block polymers, this minimum occurs at $q = q_m \sim 1/R_g$; thus χ_s is given by eq I-6. That is, χ_s is extracted from the numerical solutions of $I(q_m)^{-1}$ for the special case of $\chi = 0$. In the case of blends of block polymers, the minimum of $S(q)/W(q)$ can, in principle, occur both at $q = 0$ and at $q = q_m \neq 0$. The former gives the criterion for the spinodal point $\chi_{s, \text{macro}}$ for the macroscopic phase separation between the two (block) polymers

$$S(q=0)/W(q=0) = 2\chi_{s, \text{macro}} \quad (\text{IV-1})$$

whereas the latter gives the criterion for the spinodal point $\chi_{s, \text{micro}}$ for the microphase separation

$$S(q_m)/W(q_m) = 2\chi_{s, \text{micro}} \quad (\text{IV-2})$$

χ_s defined in eq I-6 corresponds to $\chi_{s, \text{micro}}$, and we use χ_s instead of $\chi_{s, \text{micro}}$ for discussion in this paper.

The effects of nonzero χ values may be summarized as follows. The χ value affects the scattered intensity maximum $I(q_m)$ and hence the breadth of the scattering profile; the larger the χ value, the sharper is the scattering maximum. The χ value may be determined by fitting the experimental and theoretical profiles, as described in detail elsewhere¹ and in section V in this paper. No further details on the effect of χ on the calculated scattering profiles will be given in this section.

4-1. Binary Mixtures of Block Polymers: A-B1 + A-B2. Figure 5 shows the calculated scattering profiles for the binary mixtures of A-B1 having a given DP = N_1

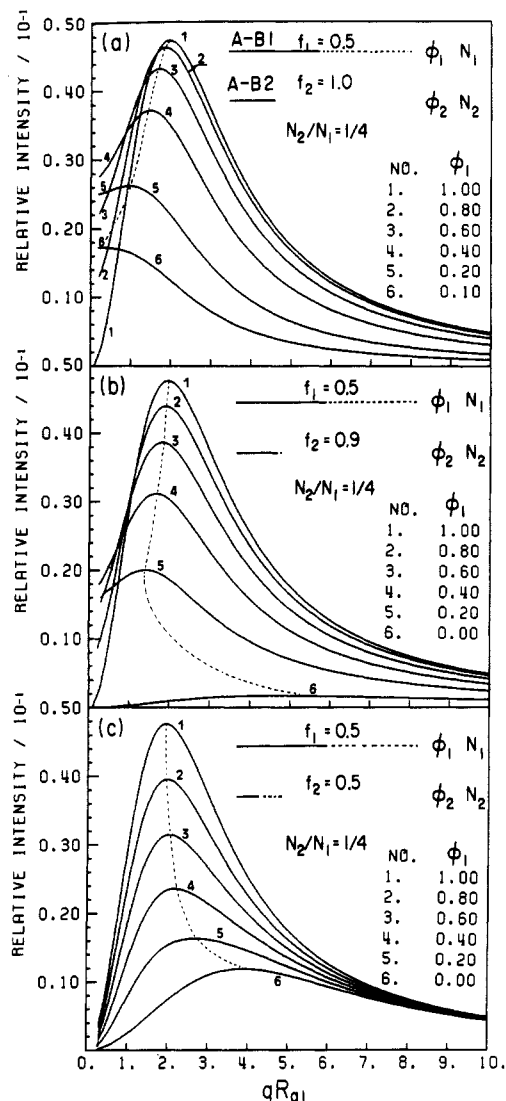


Figure 5. Scattering profiles of binary mixtures of block polymers A-B1 and A-B2 in the disordered state (case of $\chi = 0$): (a) $f_1 = 0.5$, $f_2 = 1.0$ (A homopolymer), and $N_2/N_1 = 1/4$; (b) $f_1 = 0.5$, $f_2 = 0.9$, and $N_2/N_1 = 1/4$; (c) $f_1 = f_2 = 0.5$ and $N_2/N_1 = 1/4$.

and fraction $f_1 = 0.5$ and A-B2 having a fixed DP = $N_2 = N_1/4$ but varying f_2 (see Figure 3 for notations). The profiles are calculated for various fractions ϕ_1 of A-B1 in the mixture and are plotted as a function of a reduced scattering vector qR_{g1} , where

$$R_{g1}^2 = N_1 a^2 / 6 \quad (\text{IV-3})$$

is the unperturbed radius of gyration of A-B1.

Figure 5a shows a special case where A-B2 is equal to homopolymer A (i.e., $f_2 = 1.0$). As the fraction of homopolymer with lower molecular weight increases (i.e., as ϕ_1 decreases), (i) the q_m value continuously decreases and hence the wavelength ξ continuously increases, (ii) the peak scattered intensity I_m continuously decreases and hence the spinodal point¹⁷ (χN_1)_s of the mixtures continuously increases (see eq I-1 and IV-2), suggesting increasing miscibility of the polymers,¹⁸ and (iii) the intensity at $q = 0$, i.e., $I(0)$, and hence osmotic compressibility κ_{osmo} first increase and then decrease.²⁸ The first increase of $I(0) \sim \kappa_{\text{osmo}}$ is a consequence of adding homopolymers A, and the latter decrease is a consequence of the mixture approaching a homogeneous system consisting of only homopolymer A.

The change of $I(0)$ and κ_{osmo} with ϕ_1 can be interpreted as follows. From eq III-21 to III-23 for a binary mixture

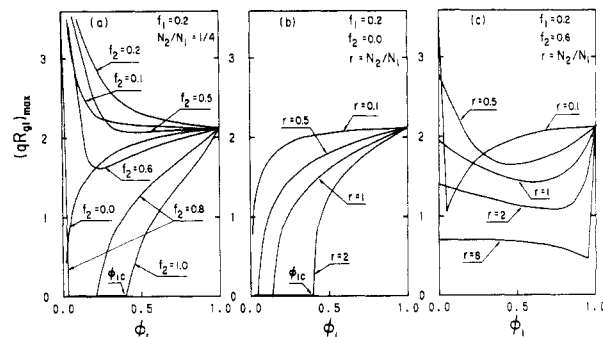


Figure 6. Reduced wavenumber $(qR_{g1})_{\text{max}}$ of the dominant mode of the fluctuations in the disordered state as a function of ϕ_1 for binary mixtures of block polymers A-B1 and A-B2: (a) results for various sets of ($f_1 = 0.2$, f_2) for $N_2/N_1 = 1/4$ (results for (f_1 , f_2) are identical with those for $(1 - f_1, 1 - f_2)$); (b, c) results for various values of $r = N_2/N_1$ and a fixed set of $f_1 = 0.2$ and $f_2 = 0$ (b) and a fixed set of $f_1 = 0.2$ and $f_2 = 0.6$ (c). ϕ_{1c} is the critical concentration below which q_m becomes zero.

of the two block polymers A-B1 and A-B2, one obtains the scattered intensity $I(0)$ in the limit of $q = 0$ by noting that

$$g(f_1, N) = f^2 - \frac{1}{3} f^2 x + \dots \quad (\text{IV-4})$$

$$I(0)^{-1} \sim \frac{S(q=0)}{W(q=0)} - 2\chi = \frac{1}{(f_1 - f_2)^2} \frac{\phi_1 N_1 + (1 - \phi_1) N_2}{\phi_1 (1 - \phi_1) N_1 N_2} - 2\chi \quad (\text{IV-5})$$

Thus the change of $I(0)$ and hence κ_{osmo} with ϕ_1 is primarily determined by the factor $\phi_1(1 - \phi_1)$, and the finite osmotic compressibility of the mixture is a consequence of the offset of the chemical composition; i.e., $f_1 - f_2 \neq 0$.

When the lower molecular weight block polymer A-B2 has a chemical composition much different from that of A-B1, as in the case of Figure 5b ($f_1 = 0.5$ and $f_2 = 0.9$), peculiar changes of q_m and ξ occur with decreasing ϕ_1 . With decreasing ϕ_1 , the q_m value first decreases and hence ξ increases as in the case of adding homopolymer (Figure 5a). However, a further decrease of ϕ_1 increases the q_m value and hence decreases the ξ value toward the values q_{m2} and ξ_2 relevant to the pure block polymer A-B2. Variations of I_m and hence $(\chi N_1)_s$ and variations of $I(0)$ and hence κ_{osmo} with ϕ_1 have the same trend as those for the mixtures of A-B1 and A (Figure 5a), except for the behavior at very small ϕ_1 .

When A-B2 has the same chemical composition f_2 as for A-B1 (Figure 5c), the peak position q_m continuously increases and hence ξ decreases with decreasing ϕ_1 from the values q_{m1} and ξ_1 relevant to pure A-B1 to those q_{m2} and ξ_2 relevant to pure A-B2. The peak intensity continuously decreases and hence $(\chi N_1)_s$ continuously increases, suggesting again enhanced miscibility with decreasing ϕ_1 . The intensity $I(0)$ or κ_{osmo} stays always zero irrespective of ϕ_1 since A-B1 and A-B2 have the same chemical composition, $f_1 = f_2$. This is clearly understood from eq IV-5.

Figure 6 shows variations of the "reduced characteristic wavenumber" $(qR_{g1})_{\text{max}} = 2\pi R_{g1}/\xi$ with ϕ_1 , R_{g1} being the unperturbed radius of gyration of block polymer A-B1. Figure 6a presents cases where A-B1 has a fixed chemical composition $f_1 (=0.2)$ and DP ($=N_1$) and A-B2 has a fixed DP of $N_2 = N_1/4$ but varying f_2 . The values $(qR_{g1})_{\text{max}} = 2\pi R_{g1}/\xi$ are plotted as a function of ϕ_1 for various values of f_2 . It should be noted that the $(qR_{g1})_{\text{max}}$ vs. ϕ_1 curve for a given set of $f_1 = 0.2$ and f_2 is identical with that for $f_1 = 0.8$, $1 - f_2$ because of the symmetry of the block polymer mixtures. The various curves have a common intercept

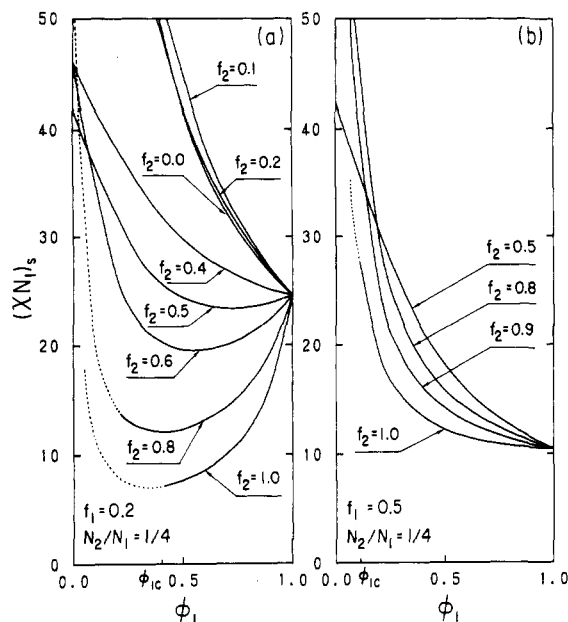


Figure 7. Spinodal point $(\chi N_1)_s$ as a function of ϕ_1 for binary mixtures of block polymers A-B1 and A-B2 with a fixed value of $r = N_2/N_1 = 1/4$: (a) $f_1 = 0.2$; (b) $f_1 = 0.5$. The broken curves represent $(\chi N_1)_{s, \text{macro}}$ (see text, eq IV-1 and IV-2).

at $\phi_1 = 1$, i.e., $(qR_{g1})_{\text{max}}$ for pure block polymer A-B1, while they do not have a common intercept at $\phi_1 = 0$. The intercept, i.e., q_{max} , for A-B2 depends on f_2 , being minimum for $f_2 = 0.5$ and diverging to infinity as $f_2 \rightarrow 0$ or 1, as is well described by Leibler.²

When $f_2 \simeq f_1 = 0.2$ (i.e., for $f_2 = 0.1$ and 0.2), $(qR_{g1})_{\text{max}} = 2\pi R_{g1}/\xi$ tends to increase continuously with decreasing ϕ_1 from 1 to 0. However, when f_2 is different from f_1 (i.e., for $f_2 = 0.5, 0.6$, and 0.8), the behavior is very peculiar: $(qR_{g1})_{\text{max}}$ first decreases with decreasing ϕ_1 from 1 and then increases with a further decrease of ϕ_1 to the value expected for pure block polymer A-B2. When $f_2 = 0$ or 1, $(qR_{g1})_{\text{max}}$ continuously decreases from the value expected for A-B1 to zero with decreasing ϕ_1 from 1 to zero. $(qR_{g1})_{\text{max}}$ becomes zero below the critical composition ϕ_{1c} , which depends on f_2 for a given N_2/N_1 ($\phi_{1c} = 0.42$ for $f_2 = 1.0$ and $\phi_{1c} = 0.23$ for $f_2 = 0.8$). ϕ_{1c} gives a criterion below which no microphase separation will occur.

Figure 6b presents some effects on $(qR_{g1})_{\text{max}}$ of adding homopolymer B with various DP's to block polymer A-B1. The greater the DP of the homopolymer, the faster the decrease of $(qR_{g1})_{\text{max}}$ with decreasing ϕ_1 and the larger the critical composition ϕ_{1c} below which $(qR_{g1})_{\text{max}}$ becomes zero. $\phi_{1c} = 0.42, 0.13$, and 0.05 for $r = 2, 1$, and 0.5 , respectively. Figure 6c presents some effects of adding block polymer A-B2 with a fixed chemical composition $f_2 = 0.6$ but with various DP's to the block polymer A-B1 with a given DP and f_1 . The figure indicates how the peculiar shift of the peak position with ϕ_1 depends on $r = N_2/N_1$. The fraction $\phi_1 (= \phi^*)$ at which the mixture attains the minimum value of $(qR_{g1})_{\text{max}}$, i.e., the maximum wavelength ξ , depends on r . The greater the value N_2 relative to the value N_1 , the larger the value ϕ_1^* .

Figure 7 shows the spinodal point¹⁷ $(\chi N_1)_s$ as a function of ϕ_1 , i.e., the volume fraction of A-B1 in mixtures of A-B1 and A-B2. Figure 7a presents $(\chi N_1)_s$ for the mixture in which A-B1 has a fixed $f_1 = 0.2$ and A-B2 has various values of f_2 but a fixed N_2 ($N_2/N_1 = 1/4$), while Figure 7b presents $(\chi N_1)_s$ for the mixture in which A-B1 has a fixed $f_1 = 0.5$ and A-B2 has various values of f_2 but a fixed N_2 ($N_2/N_1 = 1/4$). It should be noted that for mixtures with a large value of f_2 the scattering maximum at $q_m \neq 0$

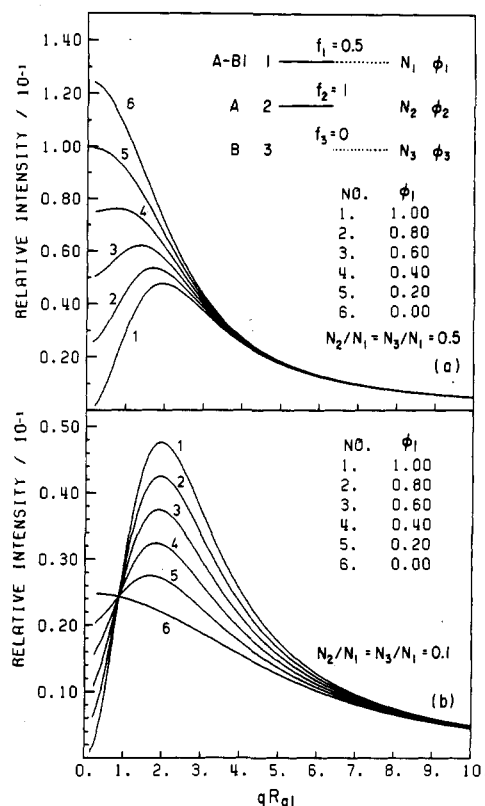


Figure 8. Scattering profiles for ternary mixtures of A-B1, A, and B with $r = N_2/N_1 = N_3/N_1$ and $f_1 = 0.5$ ($\chi = 0$). The mixtures were prepared along the isopleth line: $\phi_2 = \phi_3 = (1 - \phi_1)/2$. (a) $r = 1/2$; (b) $r = 1/10$.

disappears at $\phi_1 < \phi_{1c}$ (Figure 6a). Consequently, $\chi_s = \chi_{s, \text{micro}}$ in eq IV-2 can be determined only at $\phi_1 > \phi_{1c}$. At the composition $\phi_1 < \phi_{1c}$, the maximum of $I(q; \chi = 0) = [S(q)/W(q)]^{-1}$ exists at $q = 0$, from which one can estimate $\chi_{s, \text{macro}}$ by using eq 1. The broken curves in Figure 7 at $\phi_1 < \phi_{1c}$ correspond to $(\chi N_1)_{s, \text{macro}}$ as a function of ϕ_1 .

When smaller molecular weight block polymer A-B2 with $f_2 = f_1 (= 0.2)$ is added, $(\chi N_1)_s$ continuously increases with increasing fraction of A-B2, i.e., with decreasing ϕ_1 ; i.e., the miscibility is enhanced¹⁸ by increasing the fraction of A-B2. $(\chi N_1)_s$'s are generally smaller for mixtures of A-B1 and A-B2 with different chemical compositions ($f_1 \neq f_2$) than for those with matched compositions $f_1 \simeq f_2$. This fact is clearly manifested in Figure 7 by the fact that most of the lines exist below the lines for mixtures with matched compositions, except for the region $\phi_1 \simeq 0$. If the offset of the compositions is very large as in the case of $0.6 < f_2 < 1$ in Figure 7a, the $(\chi N_1)_s$ values show a peculiar change with ϕ_1 ; as ϕ_1 decreases, i.e., as smaller molecular weight block polymer A-B2 is added, $(\chi N_1)_s$ first decreases and then increases. This manifests itself as a peculiar change of the order-disorder transition with ϕ_1 . The fraction ϕ_1 where $(\chi N_1)_s$ becomes minimum depends on f_2/f_1 . The peculiar effect seems to depend upon f_2, f_1 , and N_1/N_2 and does not appear in the case of Figure 7b.

4-2. Ternary Mixtures: A-B + A + B. Figure 8 presents scattering profiles of ternary mixtures of symmetric block polymer A-B1 with $f_1 = 0.5$ and N_1 , A homopolymer with N_2 , and B homopolymer with $N_3 = N_2$. The mixtures are prepared along the isopleth line satisfying $\phi_2 = \phi_3 = (1 - \phi_1)/2$, the fractions of A and B monomers being always kept constant. Figure 8 shows the effect of homopolymer molecular weights relative to that of the block polymer; (a) $N_2/N_1 = N_3/N_1 = 1/2$ and (b) $N_2/N_1 = N_3/N_1 = 1/10$.

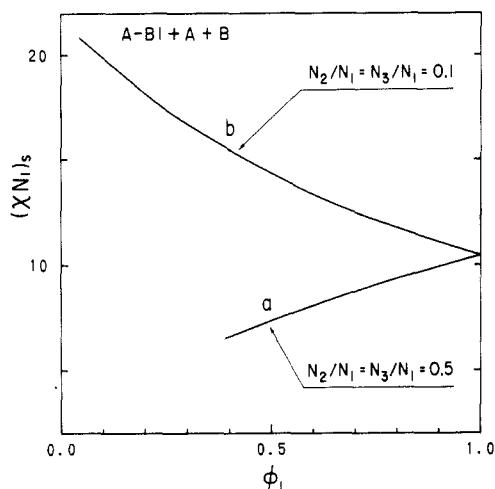


Figure 9. Spinodal point $(\chi N_1)_s$ as a function of ϕ_1 for the ternary mixtures in Figure 8. Curves a and b were obtained for $r = N_2/N_1 = 1/2$ and $1/10$, respectively.

As homopolymers are added, the scattering maximum shifts toward smaller angles, indicating the wavelength of the concentration fluctuation increases with increasing homopolymer fraction. The scattering maximum increases as homopolymers with moderate molecular weights $N_2 = N_3 = (1/2)N_1$ are added (Figure 8a), but it decreases as homopolymers with small molecular weights $N_2 = N_3 = (1/10)N_1$ are added (Figure 8b). The major difference between the two cases may reflect the molecular weight dependence of the thermal concentration fluctuations of the A/B mixtures (cf. curves numbered 6 in parts a and b of Figure 8).

Figure 9 shows $(\chi N_1)_s$ for the two ternary systems as discussed in Figure 8, curves a and b corresponding to the cases of Figure 8a and Figure 8b, respectively. $(\chi N_1)_s$ decreases and increases as homopolymers with moderate and very small molecular weights, respectively, are added, which, in turn, suggests *reduced and enhanced miscibility*¹⁷ with the addition of homopolymers. The value of $(\chi N_1)_s$ that corresponds to $(\chi N_1)_{s, \text{micro}}$ as defined in eq IV-2 does not exist at small ϕ_1 , because as seen in Figure 8 the scattering maximum does not exist at $q = q_m \neq 0$ at small ϕ_1 .

4-3. Triblock Polymers A-B-A in Comparison with Diblock Polymers A-(1/2)B. Here we compare the fluctuations occurring in the bulk disordered phases for A-B-A triblock polymer and A-(1/2)B diblock polymer, i.e., the diblock polymer obtained by cutting the triblock polymer at the center of the middle block B. Figure 10 shows scattering profiles for A-B-A triblock polymer, A-(1/2)B diblock polymer, and the triblock polymer (designated (A-B-A)/2) with the same chemical composition but with a molecular weight half that of A-B-A, all for the case where $\chi = 0$. All the block polymers have the same chemical composition $f = 0.8$ but different molecular weights.

As expected from theory (see eq III-7 and III-13 for the case of $\chi = 0$), the reduction of molecular weight by a factor of 2 causes an intensity reduction by the same factor and an increase of q_m (i.e., the peak position) by a factor of $2^{1/2}$ (see eq III-5 and III-7) as seen in Figure 10 (cf. the profiles for A-B-A and (A-B-A)/2). The latter follows simply because

$$q_m^2 \sim R_g^{-2} \sim N^{-1} \quad (\text{IV-6})$$

The wavelength ξ of the dominant mode of fluctuations or the wavenumber q_m for A-B-A triblock polymer and A-(1/2)B diblock polymer should have different values in

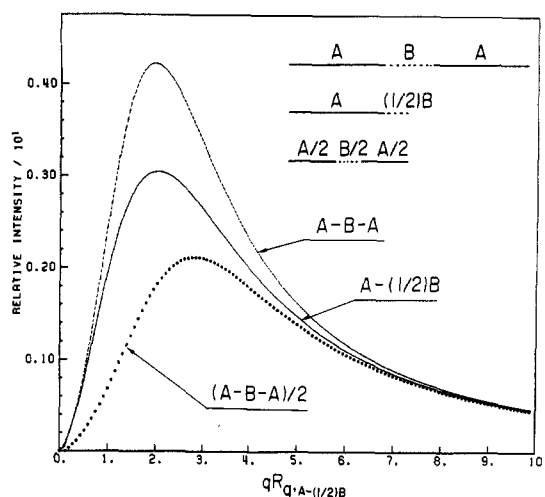


Figure 10. Scattering profiles for A-B-A, A-(1/2)B, and (A-B-A)/2 with a fraction of A block 0.8 in the disordered state ($\chi = 0$). A-(1/2)B corresponds to a diblock polymer obtained by cutting A-B-A triblock polymer in the middle of B, and (A-B-A)/2 corresponds to a triblock polymer having half the molecular weight of A-B-A but a chemical composition identical with that of A-B-A.

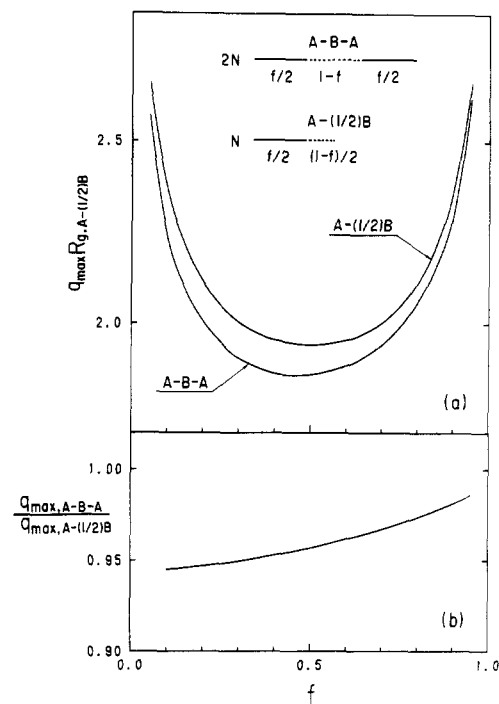


Figure 11. (a) Composition dependence of the reduced wavenumber $q_{\max} R_{g,A-(1/2)B}$ of the dominant mode of the fluctuations in the disordered state for A-B-A triblock polymer and A-(1/2)B diblock polymer and (b) composition dependence of the ratio $q_{\max,A-B-A}/q_{\max,A-(1/2)B}$. q_{\max} in the figure corresponds to q_m in the text.

principle. However, it is interesting to note that the difference is surprisingly small; the ratio of q_m for A-B-A to that for A-(1/2)B ($q_{\max,A-B-A}/q_{\max,A-(1/2)B}$) was 0.97 for the particular volume fraction of A ($f = 0.8$). Comparisons between the two cases for other f are shown in Figure 11, where q_m for A-B-A and A-(1/2)B ($q_{\max,R_{g,A-(1/2)B}}$) (Figure 11a) and the ratio $q_{\max,A-B-A}/q_{\max,A-(1/2)B}$ (Figure 11b) are plotted as a function of f . The change of q_m with f is symmetric about $f = 1/2$ for A-(1/2)B diblock polymer but is asymmetric for A-B-A, as one expects. q_m for A-B-A is only slightly smaller than that for A-(1/2)B.

It is interesting to note that A-B-A triblock polymer forms approximately and practically the same wavelength

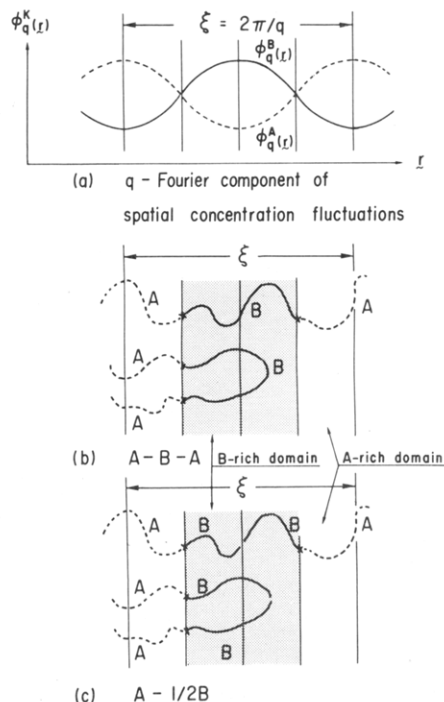


Figure 12. (a) q -Fourier component of spatial concentration fluctuations for segment A, $\phi_q^A(r)$, and segment B, $\phi_q^B(r)$, in the disordered state, and schematic illustrations of "dynamic aggregates" relevant to the q -Fourier component for A-B-A triblock polymer (b) and to that for A-(1/2)B diblock polymer (c). In the disordered state, the dynamic aggregates are not stable statically and exist in dynamic equilibrium between their formation and dissolution. The shaded and unshaded areas correspond to B-segment-rich and A-segment-rich domains, respectively, in the bulk disordered state.

$\xi = 2\pi/q_m$ as that of A-(1/2)B diblock polymer. A possible interpretation is schematically illustrated in Figure 12, where a particular Fourier mode of the thermal concentration fluctuations with the wavelength ξ is shown; (a) designates the spatial concentration fluctuations of the A and B segments in the particular mode $\phi_q^K(r)$ ($K = A$ or B), and (b) and (c) represent the "dynamical aggregations" for A-B-A and A-(1/2)B diblock polymers in the disordered state, respectively, relevant to the particular mode of the fluctuations as shown in Figure 12a. It should be noted that the formation and dissolution of the aggregates as schematically drawn in parts b and c of Figure 12 are in dynamic equilibrium in the disordered state. Parts b and c of Figure 12 represent dynamically formed A-rich (unshaded region) and B-rich domains (shaded region). Only two B blocks and four A blocks are drawn schematically to represent packing and molecular conformations of A and B blocks in each domain in the bulk disordered phase. Needless to say, in reality many block chains are participating and interpenetrating each other in the domains. It may be intuitively obvious from part b and c of Figure 12 that the wavelengths of the thermal fluctuations for the A-B-A triblock and the A-(1/2)B diblock can be practically identical; the only difference between parts b and c of Figure 12 may be seen in the connectivity of the middle part of the B chains. The connectivity gives rise to principally important but practically minor difference in q_m . A similar rule is applied also for the block polymer in the ordered state; the spacing of the microdomain formed by A-B-A is approximately the same as that formed by A-(1/2)B.

Figure 13 compares the χ -parameter at spinodal points χ_s for A-B-A and A-(1/2)B block polymers. The A-(1/2)B block polymers have the same f as the A-B-A but have

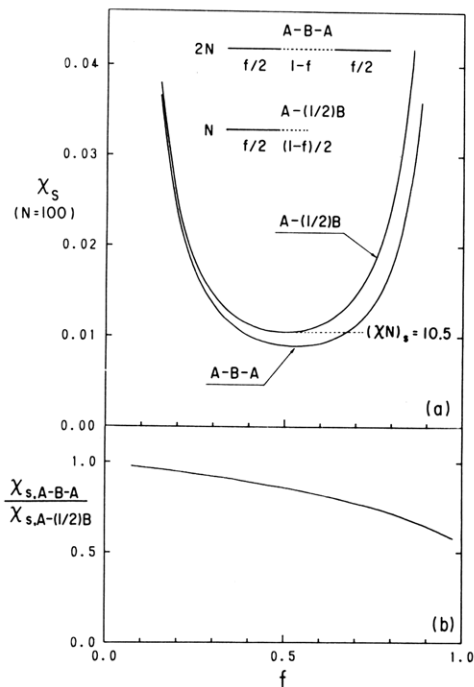


Figure 13. Comparisons of the spinodal points χ_s between A-B-A and A-(1/2)B block polymers: (a) phase diagram for $N = 100$; (b) ratio of $\chi_{s,A-B-A}$ for A-B-A to $\chi_{s,A-(1/2)B}$ for A-(1/2)B. Diblock polymer A-(1/2)B is obtained by cutting triblock polymer A-B-A in the middle of the B-block chain.

a DP half that for the A-B-A.¹⁹ One can obtain several pieces of important information from the figures. (i) First of all, the χ_s values for A-B-A and A-(1/2)B at a given f are approximately equal, indicating that the spinodal point of A-B-A is approximately equal to that of A-(1/2)B, especially when f is small. This is quantitatively presented in Figure 13b, where the ratio of χ_s for A-B-A to that for A-(1/2)B is plotted as a function of f . (ii) Secondly, the composition dependence of χ_s is asymmetric about $f = 1/2$ for A-B-A but symmetric for A-(1/2)B (Figure 13a). Obviously the asymmetry comes from the asymmetry in the molecular architecture, B in A-B-A being connected with A at both ends and A being connected with B only at one end. In other words, A-B-A with a given f is not identical with B-A-B with the same f . However, A-B with a given f is identical with B-A with the same f ; thus diblock polymer is symmetric in the molecular architecture. (iii) Owing to the asymmetry, the difference of χ_s and therefore the spinodal temperature T_s between A-B-A and A-(1/2)B is larger for A-rich polymer ($f > 0.5$) than for A-poor polymer ($f < 0.5$) (Figure 13b). (iv) χ_s for A-B-A is always smaller than that for A-(1/2)B.

4-4. Single-Phase System vs. Two-Phase System.

Here we consider mixtures of A-B diblock polymers and compare the following cases in Figure 14: (a) the two block polymers are in a disordered state and molecularly mixed (see Figure 14a; designated as a "single-phase system") and (b) the two block polymers are in a disordered state but separated in two liquid phases (see Figure 14b; designated as a "two-phase system"). We are interested in whether the two systems are distinguishable or not in terms of the scattering profiles.

In the former case as shown in Figure 14a the intensity $I(q)$ is given by the equations discussed in section 3-3, but in the latter case the intensity is given by a weighted average of two disordered liquid phases

$$I(q) = \phi_1 I_1(q) + (1 - \phi_1) I_2(q) \quad (\text{IV-7})$$

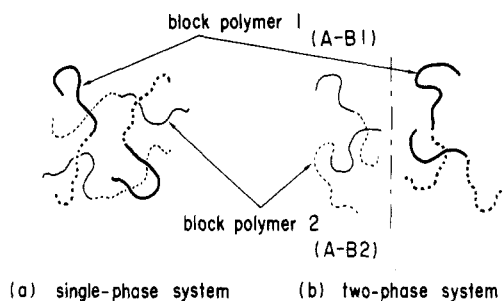


Figure 14. Schematic diagram showing two possible states of binary mixtures of block polymers A-B1 and A-B2 in the disordered state: (a) single-phase system; (b) two-phase system.

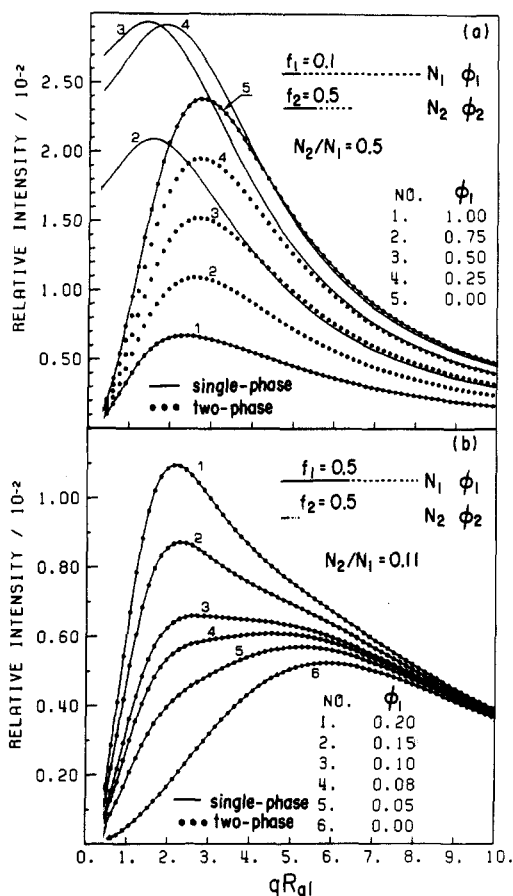


Figure 15. Scattering profiles for binary mixtures of block polymers A-B1 and A-B2 ($\chi = 0$). The solid lines correspond to the profiles for single-phase systems, and the curves represented by filled circles correspond to those for two-phase systems. (a) $f_1 = 0.1$, $f_2 = 0.5$, and $N_2/N_1 = 1/2$. (b) $f_1 = f_2 = 0.5$ and $N_2/N_1 = 0.11$.

where ϕ_i is the volume fraction of one of the liquid phases and I_i is the scattering intensity from i th liquid phase ($i = 1$ or 2). The i th liquid phase generally contains both the block polymers 1 and 2. However, we assume here for simplicity that the i th phase contains only the i th block polymer for the numerical calculations. In this case $\phi_i = \phi_i$, the volume fraction of the i th block polymer in the mixtures.

Figure 15 compares the scattering profiles from the two systems, i.e., the disordered "single phase" (the profiles drawn by solid lines) and the disordered "two-phase" (the profiles drawn by the filled circles) ($\chi N_1 = 0$). Figure 15a presents a comparison of the two cases in which the two block polymers have different compositions, i.e., $f_1 \neq f_2$, while Figure 15b presents a comparison of them in which they have identical composition, i.e., $f_1 = f_2 = 0.5$.

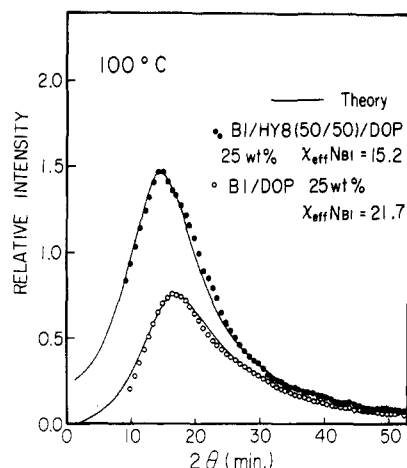


Figure 16. Small-angle X-ray scattering (SAXS) from a binary mixture of polystyrene-*b*-polyisoprene (SI) diblock polymers B1 and HY8 in the disordered state. The SAXS profiles were measured at 100 °C for the mixture B1/HY8 with DOP (dioctyl phthalate) (total polymer concentration was 25 wt % and the fraction of B1 in the mixture was 0.5; profile represented by filled circles) and that for B1/DOP (polymer concentration was 25 wt %; profile represented by open circles). The best-fitted theoretical curves are drawn by the solid lines. Cu K α radiation. 2θ is the scattering angle denoted by θ in the text.

From the figures it is obvious that the two cases, the single-phase system and the two-phase system, are in principle distinguishable for mixtures with $f_1 \neq f_2$ (Figure 15a) but indistinguishable for those with $f_1 = f_2$ (Figure 15b).²⁰ In the two-phase system, the scattering profile always changes continuously with ϕ_1 between the profiles of the block polymer 1 and the block polymer 2, the peak position and intensity being changed between those of the two block polymers. However, in a single-phase system this is not necessarily so, depending on asymmetry in the composition and molecular weight as shown in Figure 15a and as discussed in detail in section 4-1 as the "peculiar behavior".

V. Comparisons with Experimental Profiles

In this section we compare experimental SAXS (small-angle X-ray scattering) profiles from the disordered state with theoretical profiles discussed in sections III and IV.

5-1. Binary Mixture of Block Polymers: A-B1 + A-B2. The SAXS profiles from a binary mixture of SI diblock polymers of B1 and HY-8 were investigated, and typical results are shown in Figure 16. Block polymer B1 has number-average molecular weight $M_n = 8.2 \times 10^4$, heterogeneity index $M_w/M_n = 1.15$ (M_w being weight-average molecular weight), and PS weight fraction $W_{PS} = 0.83$. HY-8 has $M_n = 3.16 \times 10^4$, $M_w/M_n = 1.07$, and $W_{PS} = 0.48$. Figure 16 shows the SAXS profile at 100 °C for a binary mixture of B1 and HY-8 with $\phi_1 = \phi_2 = 0.5$ in dioctyl phthalate (DOP) (the profile shown with solid circles) and that from B1 in DOP (the profile shown with open circles). The total polymer concentration in DOP solution is 0.25 by weight for the both cases, and DOP is a neutrally good solvent for both PS and PI, which reduces the χ parameter between PS and PI to the value $\chi_{eff} = \chi\phi_p$, ϕ_p being the volume fraction of the polymer in the solution, and hence the order-disorder transition temperature.²¹

From a series of studies on the temperature dependence of the SAXS profiles, both profiles were confirmed to be those from the disordered state.¹³ The relevant experimental evidence is that (i) q_m 's are independent of tem-

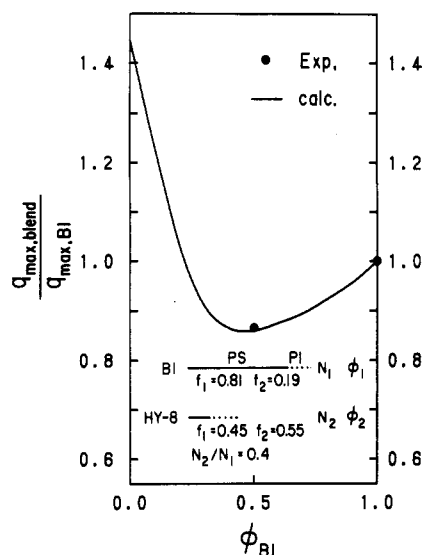


Figure 17. Predicted variation of the peak position of the binary mixture, $q_{\max, \text{blend}}$, of the block polymers relative to that of the pure block polymer B1 with ϕ_{B1} (solid line). The solid circles correspond to the data points (see Figure 16). ϕ_{B1} is the volume fraction of the block polymer B1.

perature and (ii) I^{-1} linearly decreases with T^{-1} . The solid lines in Figure 16 show the theoretical profiles best fitted with the experimental profiles, indicating a reasonable agreement between the theoretical and experimental results. The theoretical profiles were calculated by applying the equations developed for the binary mixtures of the block polymers in bulk (e.g., eq I-1, I-3, I-4, and III-21 to III-23) to the solutions with the neutral solvent. The applications involve a replacement of χ for bulk by χ_{eff} for the solution.²¹⁻²³ From the best fitting, the following parameters are obtained: $\chi_{\text{eff}} N_{B1} = 15.2$ for B1/HY8/DOP and 21.7 for B1/DOP, and $q_m R_{g, B1} = 1.83$ for B1/HY-8/DOP and 2.13 for B1/DOP, where N_{B1} and $R_{g, B1}$ are the DP and the radius of gyration of B1, respectively, and χ_{eff} is the effective χ -value between PS and PI in the presence of DOP. Figure 17 shows the predicted composition (ϕ_{B1}) dependence of the peak position of the blend $q_{\max, \text{blend}}$ relative to that of the block polymer B1, $q_{\max, B1}$ (solid line). The solid circles in Figure 17 represent the experimental data. The theoretical result in Figure 17 (solid curve) clearly supports a peculiar experimental trend that the peak position q_m shifts toward smaller angles with the addition of the block polymer, which by itself has a higher q_m .

5-2. Mixtures of Block Polymers and Homopolymers: A-B + A and A-B + A + B. Figure 18a shows an experimental SAXS profile (represented with the filled circles) for a binary mixture of HY-8 and homopolystyrene (HS) with $M_n = 2.3 \times 10^3$ and $M_w/M_n = 1.10$ and weight fraction of the block polymer (ϕ_1) 0.2. The SAXS profile was measured at 160 °C, where the mixture was known to be molecularly mixed and in the disordered state.¹⁴ Figure 18b shows an experimental SAXS profile (represented with filled circles) for a ternary mixture of HY-8, HS, and homopolyisoprene (HI) with $M_n = 3.7 \times 10^3$ and $M_w/M_n = 1.19$. The same HS as in Figure 18a was used, and the weight fractions of the block polymer, HS, and HI are 35, 32.5, and 32.5, respectively. The profile was measured at 210 °C, where the mixture was known again to be molecularly mixed and in the disordered state.¹⁴

In Figure 18, the solid lines represent the calculated results according to eq III-32 to III-34 given in section 3-4. The results indicate again a reasonably good agreement

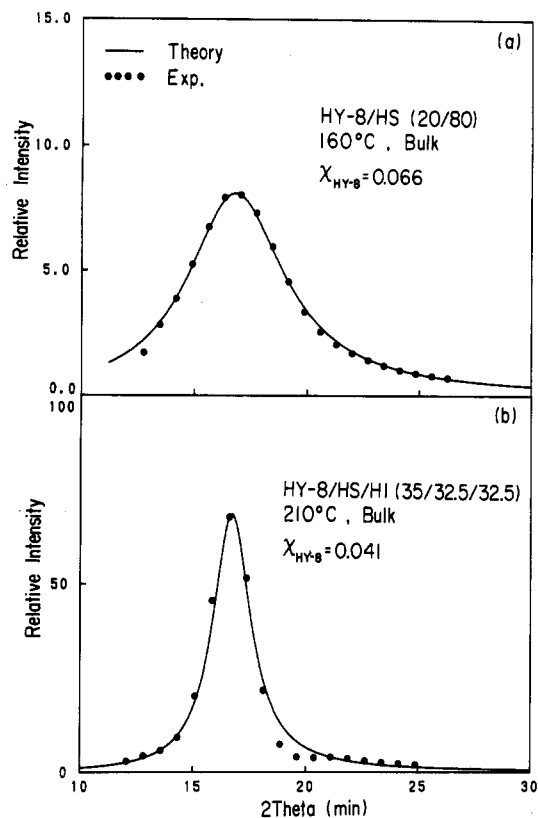


Figure 18. (a) SAXS profiles of a binary mixture of HY-8 and homopolystyrene (HS) in the disordered state. The profile represented with filled circles corresponds to that measured at 160 °C, and the solid line corresponds to the best-fitted theoretical curve. (b) The SAXS profile of a ternary mixture of SI, HS, and homopolyisoprene (HI) in the disordered state. The profile represented with filled circles corresponds to that measured at 210 °C, and the solid line corresponds to the best-fitted theoretical curve. Cu K α radiation. 2θ is the scattering angle denoted by θ in the text.

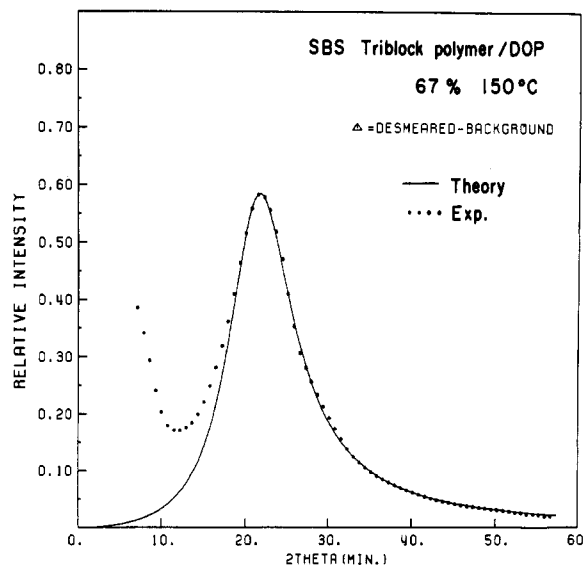


Figure 19. SAXS profile of polystyrene-*b*-polybutadiene-*b*-polystyrene (SBS) triblock polymer in the disordered state. The profile represented with filled circles corresponds to that measured at 150 °C for the DOP solution (polymer concentration being 67 wt %), and the solid line corresponds to the best-fitted theoretical curve. Cu K α radiation. 2θ is the scattering angle denoted by θ in the text.

between the measured and calculated results. The best fitting gives $R_{g, \text{HY-8}} = 80$ Å and $\chi_{SI} = 0.066$ and 0.044 at 160 and 210 °C, respectively. The physical significance

of the estimated values will be discussed elsewhere.¹⁴

5-3. Triblock Polymer. Figure 19 shows an experimental SAXS profile (represented with filled circles) for SBS triblock polymers with $M_n = 5.2 \times 10^4$ and $W_{PS} = 0.28$ in DOP, the polymer concentration being 0.67. The SAXS curve was measured at 150 °C, where the block polymer is known to be in the disordered state.¹⁵ The solid curve is calculated according to eq III-35 to III-37 given in section 3-5. The results indicate again a good agreement between the calculated and experimental profiles except for the small-angle region, smaller than the scattering $2\theta < 10$ min. The upturn of the experimental SAXS profile with decreasing 2θ may be due to parasitic scattering. The best fitting gives $R_g = 107$ Å and $\chi_{SB,eff} = 0.067$. Thus the theory turns out to be quite useful in determining the temperature dependence of χ , the wavelength of the dominant mode of concentration fluctuations (and hence chain dimensions of a single block polymer molecule in the disordered state), spinodal point for the microphase separation χ_s (i.e., the point at which $I(q_m)$ diverges), and spinodal point $\chi_{s,macro}$ for the macroscopic liquid-liquid phase separation (i.e., the point at which $I(q=0)$ diverges). The parameters estimated should be further tested by any independent measurements, which will deserve future studies.

Appendix. Derivation of Eq III-1 to III-3 for ABR1-ABR2

Let us calculate first the density-density correlation $S_{AA}(q)$ between two A monomers for a random copolymer ABR. The random copolymer has a sequence distribution of A and B monomers. We define Ω_k to be the k th sequence distribution and $P(\Omega_k)$ to be the probability of finding the k th sequence distribution. The density-density correlation $S_{AA}^k(q)$ between two A monomers for Ω_k is generally given by

$$S_{AA}^k(q) = \frac{1}{N} \sum_{i,j} \mu_i^k \mu_j^k P_{ij}(q) \quad (A1)$$

where N is the polymerization index and μ_i^k is a factor equal to unity and zero if the i th segment is A and B, respectively. The product $\mu_i^k \mu_j^k$ depends on the sequence distribution, and hence $S_{AA}^k(q)$ depends also upon the distribution. $P_{ij}(q)$ is the correlation between the i th and j th segments, i.e., the probability of finding any two segments at the i th and j th positions of a chain. We assume that P_{ij} is independent of Ω_k and is given by a Gaussian in the context of the random phase approximation

$$P_{ij}(q) \sim \exp(-y|i-j|), \quad y = q^2 a^2 / 6 \quad (A2)$$

where a is the statistical segment length.

The correlation $S_{AA}(q)$ is obtained by averaging the correlation $S_{AA}^k(q)$ over all possible Ω_k 's

$$S_{AA}(q) = \langle S_{AA}^k(q) \rangle_{\Omega_k} \equiv \sum_k P(\Omega_k) S_{AA}^k(q) \quad (A3)$$

where $\langle \rangle_{\Omega_k}$ stands for the average over all possible Ω_k 's. From eq A2 and A3

$$S_{AA}(q) = \frac{1}{N} \sum_{i,j} [\sum_k P(\Omega_k) \mu_i^k \mu_j^k] P_{ij}(q) = \frac{1}{N} \sum_{i,j} \langle \mu_i \mu_j \rangle_{\Omega_k} P_{ij}(q) \quad (A4)$$

The random copolymer defined by the IUPAC Commission on Macromolecular Nomenclature²⁵ obeys Bernoulli statistics for the sequence distribution. Hence

$$\langle \mu_i^k \mu_j^k \rangle_{\Omega_k} = \langle \mu_i^k \rangle_{\Omega_k} \langle \mu_j^k \rangle_{\Omega_k} \quad (A5)$$

and

$$\langle \mu_i^k \rangle_{\Omega_k} = \psi \quad \text{if the } i\text{th segment is A}$$

$$\langle \mu_i^k \rangle_{\Omega_k} = 1 - \psi \quad \text{if the } i\text{th segment is B} \quad (A6)$$

where ψ is the composition of A in the random copolymer. Thus

$$S_{AA} = \frac{1}{N} \sum_{i,j} \bar{\mu}_i \bar{\mu}_j P_{ij} \quad (A7)$$

$$= \frac{1}{N} \psi^2 \sum_{i,j} P_{ij} \equiv \psi^2 S_0 \quad (A8)$$

where $\bar{\mu}_i = \langle \mu_i^k \rangle_{\Omega_k}$ instead of 1 or 0 for homopolymers or block polymers.

Similarly, one obtains $S_{AB} = \psi(1 - \psi)S_0$, and $S_{BB} = (1 - \psi)^2 S_0$. Thus the scattered intensity $I(q)$ for an isolated random copolymer chain is given by

$$I(q) \sim b_A^2 S_{AA} + b_B^2 S_{BB} + 2b_A b_B S_{AB} = \bar{b}^2 S_0 \quad (A9)$$

$$\bar{b} = b_A \psi + b_B (1 - \psi) \quad (A10)$$

where b_K is the scattering power of the K th monomer. Thus $I(q)$ for the random copolymer is equal to $I(q)$ for a homopolymer with a mean scattering power \bar{b} . The scattering from bulk random copolymer systems in equilibrium becomes zero as one can expect, since

$$S(q) = S_{AA} + S_{BB} + 2S_{AB} = S_0 \quad (A11)$$

$$W(q) = S_{AA} S_{BB} - S_{AB}^2 = 0 \quad (A12)$$

By using eq A7 and keeping in mind the notations given in Figure 2, one can now calculate S_{AA} , S_{AB} , and S_{BB} for the block polymer ABR1-ABR2 as follows.

$$\begin{aligned} S_{AA} &= \frac{2}{N} \sum_{i>j} \bar{\mu}_i \bar{\mu}_j P_{ij}(q) \simeq \\ &\frac{2}{N} \int_0^{fN} \psi_1 di \int_0^i \psi_1 dj \exp[-y(i-j)] + \frac{2}{N} \int_{fN}^N \psi_2 di \int_{fN}^i \psi_2 \\ &dj \exp[-y(i-j)] + \frac{2}{N} \int_0^{fN} \psi_1 dj \int_{fN}^N \psi_2 di \exp[-y(i-j)] \end{aligned} \quad (A13)$$

The detailed calculations of eq A13 will result in eq III-1. Similarly

$$\begin{aligned} S_{BB} &= \frac{2}{N} \sum_{i>j} \bar{\mu}_i \bar{\mu}_j P_{ij}(q) \simeq \frac{2}{N} \int_0^{fN} (1 - \psi_1) di \int_0^i (1 - \psi_1) dj \\ &\exp[-y(i-j)] + \frac{2}{N} \int_{fN}^N (1 - \psi_2) di \int_{fN}^i (1 - \psi_2) dj \\ &\exp[-y(i-j)] + \\ &\frac{2}{N} \int_0^{fN} (1 - \psi_1) dj \int_{fN}^N (1 - \psi_2) di \exp[-y(i-j)] \end{aligned} \quad (A14)$$

$$\begin{aligned} S_{AB} &\simeq \frac{2}{N} \int_0^{fN} \psi_1 di \int_0^i (1 - \psi_1) dj \exp[-y(i-j)] + \\ &\frac{2}{N} \int_{fN}^N \psi_2 di \int_{fN}^i (1 - \psi_2) dj \exp[-y(i-j)] + \\ &\frac{2}{N} \int_0^{fN} (1 - \psi_1) dj \int_{fN}^N \psi_2 di \exp[-y(i-j)] \end{aligned} \quad (A15)$$

The detailed calculations of eq A14 and A15 result in eq III-2 and III-3, respectively.

Registry No. SI (block copolymer), 105729-79-1; HS (homopolymer), 9003-53-6.

References and Notes

- Mori, K.; Hasegawa, H.; Hashimoto, T. *Polym. J. (Tokyo)* **1985**, *17*, 799.
- Leibler, L. *Macromolecules* **1980**, *13*, 1602.
- de Gennes, P.-G. *Scaling Concepts in Polymer Physics*; Cornell University: Ithaca, NY, 1979.
- Leibler, L.; Benoit, H. *Polymer* **1981**, *22*, 195.

- (5) ten Brinke, G.; Karasz, F. K.; MacKnight, W. J. *Macromolecules* 1983, 16, 1827.
- (6) Kambour, R. P.; Bendler, J. T.; Bopp, R. C. *Macromolecules* 1983, 16, 753.
- (7) Paul, D. R.; Barlow, J. W. *Polymer* 1984, 25, 487.
- (8) Izumitani, T.; Hashimoto, T. *J. Chem. Phys.* 1985, 83, 3694.
- (9) Benmouna, M.; Benoit, H. *J. Polym. Sci., Polym. Phys. Ed.* 1983, 21, 1227.
- (10) Boue, F.; Daoud, M.; Nierlich, M.; Williams, C.; Cotton, J. P.; Farnoux, B.; Jannink, G.; Benoit, H.; Duplessix, R.; Picot, C.; *Neutron Inelastic Scattering, Proc. Symp.*, 1977 1978, 1, 563.
- (11) LeGrand, A. D.; LeGrand, D. G. *Macromolecules* 1979, 12, 450.
- (12) Hashimoto, T., unpublished paper.
- (13) Mori, K.; Hasegawa, H.; Hashimoto, T., to be submitted to *Macromolecules*.
- (14) Tanaka, H.; Hasegawa, H.; Hashimoto, T., to be submitted to *Macromolecules*.
- (15) Hashimoto, T.; Mori, K.; Okawara, A.; Hasegawa, H., to be submitted to *Macromolecules*.
- (16) Cahn, J. W.; Hilliard, J. E. *J. Chem. Phys.* 1958, 29, 258; 1959, 31, 688.
- (17) This refers to the spinodal point for the order-disorder transition of block polymers (microphase separation) rather than that for the liquid-liquid phase separation between the two polymers.
- (18) The enhanced miscibility is identical with the decreased order-disorder transition temperature of the block polymer systems.
- (19) The χ_s values in Figure 13a were determined for the particular case of $N = 100$ (DP of A-(1/2)B). The χ_s values for other N 's can be easily obtained by noting that $(\chi N)_s$ is invariant.
- (20) When $f_1 = f_2$, there is no thermodynamic driving force that stabilizes the two-phase structure in the disordered state; i.e., the single phase is always the thermodynamically stable structure. Therefore one does not need to worry about the distinguishability. However, it is generally concluded that the distinguishability of the two systems becomes less as the offset of the f value becomes less.
- (21) The relation $\chi_{\text{eff}} = \chi\phi_p$ is obtained from the mean-field approximation. As the concentration of polymer increases, the concentration-blob³ size tends to decrease to the segmental size. In this limit polymer A and polymer B are mixed at the segmental level so that this relation between χ_{eff} and χ becomes exactly legitimate. Here we are not concerned with the accuracy of this relation, which determines the accuracy of χ estimated by this method. We are rather concerned whether or not the experimental profiles can be fitted with the theoretical profile by using the effective $\chi(\chi_{\text{eff}})$. The problems of polymer A + polymer B + neutral good solvent can be shown to have a one-to-one correspondence to the problems of polymer A + polymer B by replacing χ (for the systems without solvent) by the effective χ value.²⁵ Of course, the scaling prediction gives a relationship^{22,23} between χ and χ_{eff} different from $\chi_{\text{eff}} = \chi\phi_p$.
- (22) de Gennes, P.-G. *J. Polym. Sci., Polym. Phys. Ed.* 1978, 16, 1883.
- (23) Onuki, A.; Hashimoto, T., in preparation.
- (24) Leibler² defined N and R_g as polymerization index and radius of gyration of the entire block chain, respectively. In this case $q_m \simeq 2/R_g$ for $f = 1/2$. However, in Figure 1, N is defined as the polymerization index of A or B rather than that of the entire block polymer A-B in order to facilitate the comparison with the polymer mixture. Hence R_g in this figure corresponds to $R_g/2^{1/2}$ defined by Leibler. The rest of this paper follows Leibler's definition of N .
- (25) IUPAC Commission on Macromolecular Nomenclature *Pure Appl. Chem.* 1985, 57, 1427.
- (26) It should be noted that Olvera de la Cruz and Sanchez developed a new type of theory based on the path-integral approach.²⁷
- (27) Olvera de la Cruz, M.; Sanchez, I. *Macromolecules* 1986, 19, 2501.
- (28) The numerical solutions were obtained down to the value $qR_{g1} = 0.03$ with good accuracy. The intensity $I(0)$ can be obtained in analytical form as in eq IV-5, from which the asymptotic behavior near $q = 0$ and its dependence on ϕ_1 are discussed.
- (29) We assume block polymer ABR1-ABR2 can be prepared by a sequential polymerization of ABR1 block and ABR2 block.

Surface Light Scattering Study of a Poly(ethylene oxide)-Polystyrene Block Copolymer at the Air-Water and Heptane-Water Interfaces

Bryan B. Sauer and Hyuk Yu*

Department of Chemistry, University of Wisconsin, Madison, Wisconsin 53706

Chao-fong Tien[†] and Douglas F. Hager

*Miami Valley Laboratories, Procter & Gamble Company, Cincinnati, Ohio 45247.
Received July 15, 1986*

ABSTRACT: Spread films of a poly(ethylene oxide)-polystyrene diblock copolymer were studied at the air-water and heptane-water interfaces by using the Wilhelmy plate technique and surface quasi-elastic light scattering (SLS) from capillary waves. At the air-water interface, the dynamic film viscoelastic parameters, i.e., surface pressure, surface dilational elasticity and viscosity, and transverse viscosity, were deduced from the SLS measurements. The static surface tension and dilational elasticity were compared to their dynamic counterparts from SLS. At the heptane-water interface, the dynamic surface pressure and transverse viscosity were evaluated, and the latter was found to be zero for the whole surface concentration range. Some speculations about possible chain conformations of the copolymer at the two interfaces are offered.

Introduction

This is a study of a nonionic surfactant representative of an important and widely used group of nonionic surfactants containing ethylene oxide linkages as the hydro-

philic component. We use here a low molecular weight sample ($M_n = 4135$) of a poly(ethylene oxide)-polystyrene block copolymer (PEO-PS). It can be spread on the air-water and heptane-water interfaces; hence the surface concentration is easily controlled (the air-water interface and heptane-water interface henceforth are referred to as A/W and O/W, respectively). A novel feature of the copolymer is the hydrophobic component, i.e., PS segments,

*Present address: Science Center, Air Products and Chemicals, Inc., Allentown, PA 18105.